ECONSTOR
Make Your Publications Visible.

A Service of

ZBW Leibniz-Informationszentrum Wirtschaft
Leibniz Information Centre for Economics

Naderloo, Leila

Article

Energy ratio of produced biodiesel in hydrodynamic cavitation reactor equipped with LabVIEW controller and artificial intelligence

Energy Reports

Provided in Cooperation with:
Elsevier

Suggested Citation: Naderloo, Leila (2020) : Energy ratio of produced biodiesel in hydrodynamic cavitation reactor equipped with LabVIEW controller and artificial intelligence, Energy Reports, ISSN 2352-4847, Elsevier, Amsterdam, Vol. 6, pp. 1456-1467, https://doi.org/10.1016/j.egyr.2020.05.029

This Version is available at:
https://hdl.handle.net/10419/244136

Standard-Nutzungsbedingungen:

Die Dokumente auf EconStor dürfen zu eigenen wissenschaftlichen Zwecken und zum Privatgebrauch gespeichert und kopiert werden.

Sie dürfen die Dokumente nicht für öffentliche oder kommerzielle Zwecke vervielfältigen, öffentlich ausstellen, öffentlich zugänglich machen, vertreiben oder anderweitig nutzen.

Sofern die Verfasser die Dokumente unter Open-Content-Lizenzen (insbesondere CC-Lizenzen) zur Verfügung gestellt haben sollten, gelten abweichend von diesen Nutzungsbedingungen die in der dort genannten Lizenz gewährten Nutzungsrechte.

Terms of use:

Documents in EconStor may be saved and copied for your personal and scholarly purposes.

You are not to copy documents for public or commercial purposes, to exhibit the documents publicly, to make them publicly available on the internet, or to distribute or otherwise use the documents in public.

If the documents have been made available under an Open Content Licence (especially Creative Commons Licences), you may exercise further usage rights as specified in the indicated licence.

https://creativecommons.org/licenses/by-nc-nd/4.0/

WWW.ECONSTOR.EU

Mitglied der Leibniz-Gemeinschaft

Energy Reports 6 (2020) 1456–1467

Contents lists available at ScienceDirect

Energy Reports

journal homepage: www.elsevier.com/locate/egyr

Research paper

Energy ratio of produced biodiesel in hydrodynamic cavitation reactor equipped with LabVIEW controller and artificial intelligence

Leila Naderloo

Mechanization Engineering of Agricultural Machinery, Department of Mechanical Biosystems Engineering, Faculty of Agriculture, College of Agriculture and Natural Science, Razi University, Kermanshah, Iran

ARTICLE INFO

Article history:
Received 24 December 2019
Received in revised form 4 May 2020
Accepted 28 May 2020
Available online xxxx

Keywords:
Biodiesel
Energy ratio
Reactor
ANN
ANFIS
RSM

ABSTRACT

This research utilized a combined hydrodynamic cavitation reactor to produce biodiesel. The reactor worked automatically with the help of a controller designed by LabVIEW. For this purpose, rapeseed oil (0.5 L per experiment) and methanol alcohol with the sodium hydroxide catalyst were used for biodiesel production. The important factors of the study were: 1.pump flow rate (three levels of 1.4, 2 and 2.6 L/min); 2.the molar ratio of methanol to oil (4:1, 6:1 and 8:1); 3.the rotational speed of the reactor (8000, 12000 and 16000 rpm), and 4.circulation time (2, 4 and 6 min). The study analyzed the energy ratio (output energy/input energy) of the produced biodiesel to evaluate the system and modeled the performance of the system to obtain the best-operating conditions of the reactor. In this respect the adaptive neuro-fuzzy inference system (ANFIS), artificial neural network (ANN) and response surface methodology (RSM) methods were employed. The average energy ratio was obtained 1.205, and the R^2 of the best ANFIS, ANN and RSM models were 0.989, 0.966, and 0.990, respectively, and MSE was calculated at 0.0005, 0.0015 and 0.00003. The results revealed that the RSM and ANFIS models were preferred to the neural network model in terms of better performance, simplicity, and high processing speed. In general, the RSM model functioned better than the ANFIS model. Accordingly, the best reactor settings to obtain the maximum energy ratio (1.35) and biodiesel yield (91.87 %) was when the circulation time, the rotational speed, the pump flow rate and the molar ratio were set at 2 min, 8000 rpm, 1.4 L/min and 4, respectively.

© 2020 The Author. Published by Elsevier Ltd. This is an open access article under the CC BY license (http://creativecommons.org/licenses/by/4.0/).

1. Introduction

Biofuels, as organic matter, are one of the major sources of renewable fuels or alternatives to fossil fuels. Biofuels mainly emit less pollution than fossil fuels (Demirbas, 2009). Diesel engines powered by biodiesel fuels have lower emissions (carbon monoxide, unheated hydrocarbons, soot and other pollutants) than diesel engines powered by diesel fuels (Gerpen, 2005).

Nowadays, most commercial biodiesel is produced worldwide through transesterification reactions in continuous-stirred tank reactors. The production of biodiesel in continuous-stirred tank reactors is accompanied by problems such as low reaction speed, long reaction time, needing much volume, weight and space for equipment, sensitivity to the quality of reaction materials, requiring energy, and being uneconomical. Therefore, the study of new and alternative technologies with the aim of intensifying the process of biodiesel fuel production is very important in terms of production efficiency, process time, energy consumption, and the quality of the produced biodiesel.

Among the innovations of biodiesel production technology, the hydrodynamic cavitation method is a high-potential method for producing biodiesel at an industrial scale that can be developed more easily (Pal et al., 2010b). This method is a cheaper conversion process and its energy requirement is approximately half the amount of energy required by the conventional mechanical method. Moreover, the speed and efficiency of the transesterification reaction are boosted through this method (Gogate and Pandit, 2005). The results of studies done by Kelkar et al. revealed that the efficiency of the energy of hydrodynamic cavitation reactors was higher than that of acoustic cavitation reactors, and their production performance was higher, too. Therefore, the effect of the intensity of the reaction in the hydrodynamic reactor is higher. At an industrial production scale, the hydrodynamic cavitation method is conducted more easily (Ji et al., 2006). In a study, Pal et al. (2010b), employed the hydrodynamic cavitation method and applied perforated plates to produce a type of biodiesel with less retention time and adequate quality.

Energy balance is the first step in evaluating raw material for the production of biodiesel. Two accepted indexes for analyzing the energy ratio and productivity of biofuels are increasing the net energy (Output energy (MJ/L) - Input energy (MJ/L)) and

E-mail address: l.naderloo@razi.ac.ir.

https://doi.org/10.1016/j.egyr.2020.05.029
2352-4847/© 2020 The Author. Published by Elsevier Ltd. This is an open access article under the CC BY license (http://creativecommons.org/licenses/by/4.0/).

the difference between the total energy outputs and total energy inputs (Nguyen and Gheewala Sh Fau - Garivait, 0000). The balance of pure biomass energy, such as biodiesel from which energy is received, is very important because it is not logical to consume more energy for its production while the produced energy is small per unit of energy consumption, otherwise the system will not remain stable. One method for analyzing sustainability issues is energy analysis. The ratio of the consumed energy to the energy produced by the product is an index for comparing systems (Mohammadshirazi et al., 2014). In a study, the energy analysis of biodiesel production from waste oil in an ultrasonic reactor was investigated and the energy ratio and productivity were obtained at 1.28 and 0.024 kg/MJ (Naderloo et al., 2017). In another study, Mohammadshirazi et al. (2014), examined the energy of the biodiesel produced from waste oil using the mechanical mixing method and estimated the energy ratio and productivity at 1.49 and 0.04 kg/MJ. In assessing the energy analysis of biodiesel production from rapeseed oil, Abshar and Sami (2016) showed that the energy ratio and productivity were obtained at 1.08 and 0.03 kg/MJ. In a study the potentiality of biodiesel production from palm oil was analyzed in Thailand and the net energy value and energy ratio were estimated at 24 MJ/kg and 2.5. It was shown that the system was completely energy-efficient (Papong et al., 2010).

In some studies, the synthesis of biodiesel from waste cooking oil (Chuah et al., 2017) and rubber seed oil (Bokhari et al., 2017) via hydrodynamic cavitation (HC) system, and non-edible sources as Pistacia Khinjuk seed oil (Asif et al., 2017a) and non-edible Salvadora Alii and Thespesia populneoides oils (Asif et al., 2017b) via ultrasonic cavitation system (UC) have been reported. Parametric optimization was done by central composite design and response surface methodology. In these researches, the performance of HC and UC at optimized values were compared with mechanical stirring (MS). HC and UC were more efficient than MS in terms of time and energy efficiency. The HC and UC showed higher reaction constant and time efficiency than MS, and the superiority of HC and UC over MS have been established in these studies.

For modeling the relationships between variables, the classical statistical methods have a number of presuppositions and limitations. For instance, some of the limitations of the classical methods include considering a default distribution, such as normal distribution for response variables, the linearity of the proposed relationships, the equivalence of the variance of errors, and so on. In addition, none of these methods can model complex non-linear relationships and high-level interactions (Khanna, 1990; Dayhoff, 1990). Today, with the rapid development of computer-processing technologies and related software, the benefits of artificial intelligence technology help us solve system-modeling problems and predict processes (Farkas et al., 2000). ANN and ANFIS are two methods of artificial intelligence technologies. For example, in a study, the energy ratio of biodiesel production from waste oil in an ultrasonic reactor was investigated by the ANFIS method (Naderloo et al., 2017). In modeling the effects of reactor size and ultrasound power on biodiesel production efficiency, Mostafaei et al. (2016) calculated the coefficient of determination in the ANFIS at model 0.981 and it was higher than the RSM ($R^2 = 0.967$). The process of producing biodiesel in a continuous microchannel was optimized by the RSM method in a study conducted by Mohadesi et al. (2017). In other studies, Hosseinpour et al. (2016), Miraboutalebi et al. (2016) and Piloto-Rodríguez et al. (2013), employed the ANN model to estimate the Cetane number of biodiesel.

Biodiesel yield is usually an important indicator in determining the optimal reactor conditions, but more energy may be used for a very small enhancement in the performance of the biodiesel, while the energy obtained is not much different. In other words, for the maximization of biodiesel yield in the reactor, the energy ratio (output energy/input energy) may be reduced, which is equivalent to more energy consumption. This will be a significant number in large-scale production. So, in this study, energy ratio rather than biodiesel yield was used for the optimization of reactor conditions because it optimizes the reactor performance both in terms of percentage of biodiesel yield and energy consumption. In this research, a hydrodynamic reactor equipped with a LabVIEW controller was used for biodiesel production. The LabVIEW controller is an important step towards the industrialization of the reactor, and it can increase the energy ratio by reducing human labor. Anyway, to find the best settings of the hydrodynamic cavitation reactor equipped with a LabVIEW controller, this study should model the performance of the reactor for producing biodiesel based on its settings. The ANFIS, ANN and RSM methods were used for this purpose due to the great power of artificial intelligence techniques in modeling, and the best reactor settings were optimized by the best model.

2. Materials and methods

In the present study, transesterification, the most commonly and commercially used method for biodiesel production, along with the alkali catalyst, was employed. Fig. 1 shows the schematic diagram of the used hydrodynamic cavitation reactor and the hydraulic and electric pathways.

As shown in Fig. 1, the rapeseed oil and methoxide were first combined with a specific ratio in the homogenizer tank, and the combination was then pumped to the reactor with a specified flow. If the temperature of the fluid exceeds the set value, the cooling system is activated and the cooling operation is performed. All steps and settings were controlled by the LabVIEW controller on the PC. The hardware interface among the computer, sensors and operators was the external NI USB DAQ6009 data card, which was connected to a computer with a USB Port. The connection of this card was only possible by the use of the software developed by LabVIEW.

2.1. LabVIEW

The overall view of the LabVIEW is shown in Fig. 2. This controlling system exploited seven electrical valves, a valve for controlling the flow rate, a switch for activating the cooling fan, a switch for activating the pump and two thermometers at the inlet and outlet of the reactor.

The algorithm of this system consisted of six separate stages: (1) pouring the rapeseed oil and methoxide with different volumetric percentages into the pre-mixing tank, (2) initial mixing, (3) the pass through the reactor operation, (4) cooling stage, (5) discharging the generated biodiesel into the final tank, and (6) discharging the final tank.

The energy index evaluated in the present study was the energy ratio (ER), which was calculated by Eq. (1) (Mandal et al., 2002; Mohammadi et al., 2010; Ju et al., 2006; Naderloo et al., 2012):

$$ER(EUE) = \frac{E_{out}(MJL^{-1})}{E_{in}(MJL^{-1})} \quad (1)$$

where E_{out} (MJ/L) and E_{in} (MJ/L) are the output and input energies, respectively. The input energy included human labor, rapeseed oil, alcohol (methanol), sodium hydroxide catalysts, electricity, and machinery. The human labor, whose energy equivalent magnitude is 1.96 MJ/h in the current study (Esengun et al., 2007), relates to the operations of the device needed by the operator, which pours the oil, alcohol and catalyst into the respective tanks and performs the monitoring and adjustments of the system

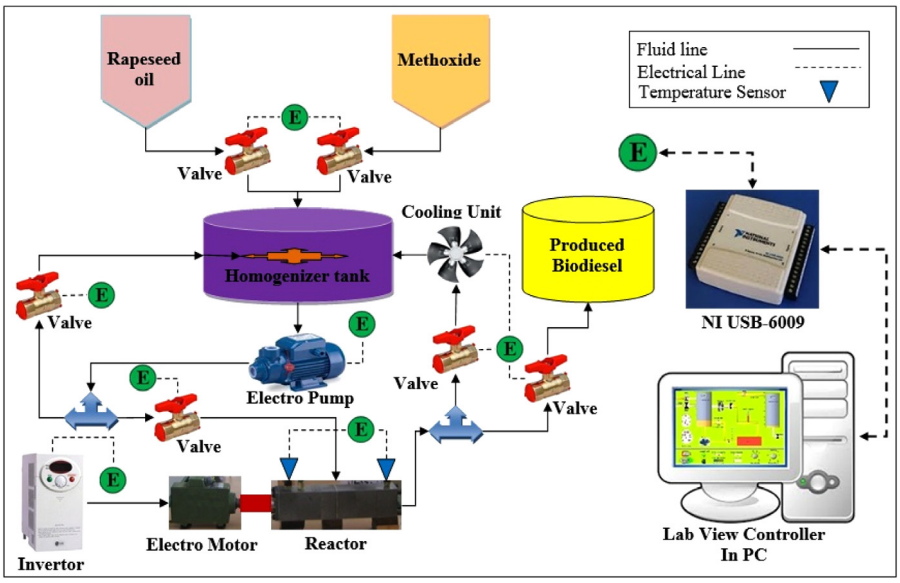

Fig. 1. The schematic diagram of the equipment of the whole system.

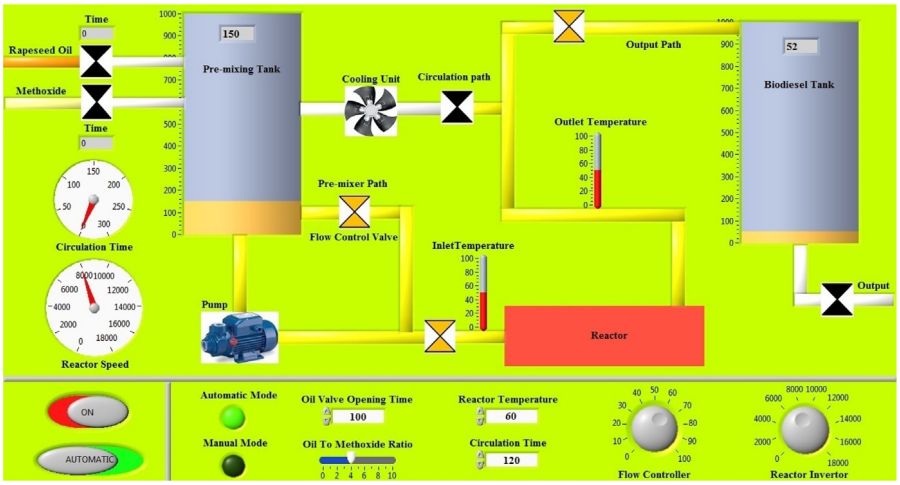

Fig. 2. The overall view of the designed LabVIEW program.

equipped with the LabVIEW controller. In addition, the efficiency of the reaction of biodiesel production was measured by the Gas chromatograph (GC) device (biodiesel production percentage in reaction). The outputs included biodiesel, methanol, catalysts, and the combination of glycerol, monoglyceride and diglyceride.

The energy equivalents of the rapeseed oil (21.7 MJ/kg) (Jafari et al., 2015), methanol (33.67 MJ/kg) (Singh and Mittal, 1992), catalyst (21.3 MJ/kg) (Kent, 2013), electricity (11.93 MJ/kwh) (Esengun et al., 2007), machine (62.70 MJ/h) (Singh, 2002), biodiesel (37.25 MJ/kg) (Saiki et al., 1999) and impure glycerin (25.30 MJ/kg) (Mohammadshirazi et al., 2014) were used for analysis. For system evaluation, it is necessary to produce biodiesel in practice and perform the requisite analyses.

In this respect, as much as 0.5 l of rapeseed oil, methanol alcohol with a purity of 99.8 percent and different molar ratios of methanol to oil and high-purity sodium hydroxide catalyst (99%) were used for each experiment. In general, the practical experiment was performed and the biodiesel measured by the GC device was analyzed. All experiments were performed at a constant temperature of 50 °C. In all of these models, the inputs included four items: pump flow rate (at three levels of 1.4, 2 and 2.6 L/min), the molar ratio of methanol to oil (at three levels of 4:1, 6:1, and 8:1), rotational speed (8000, 12000 and 16000 rpm), and circulation time (2, 4 and 6 min). The performance of the system was modeled so that the best-operating conditions of the reactor in terms of energy ratio was obtained. The ANFIS, ANN and RSM methods were employed for this purpose.

2.2. Hydrodynamic cavitation

Whenever there is a drop in the pressure of the fluid flow, and the vapor pressure is reached, the fluid boils and steam bubbles are formed and transported by the fluid flow to reach an area with a higher pressure. In this area, the bubbles are suddenly distilled. This process is referred to as cavitation. As a result of each bubble burst, there will be an inflow of the surrounding fluid to fill the cavity.

The fluid influx creates a lot of local pressure that causes the surface to corrode if the bubbles are near or in contact with the solid surface. For the determination of the sensitivity of a system to cavitation, a dimensionless quantity, namely the cavitation number, is defined as follows (Singhal et al., 2002):

$$\sigma = (p_r - p_v)/(1/2\rho v^2) \quad (2)$$

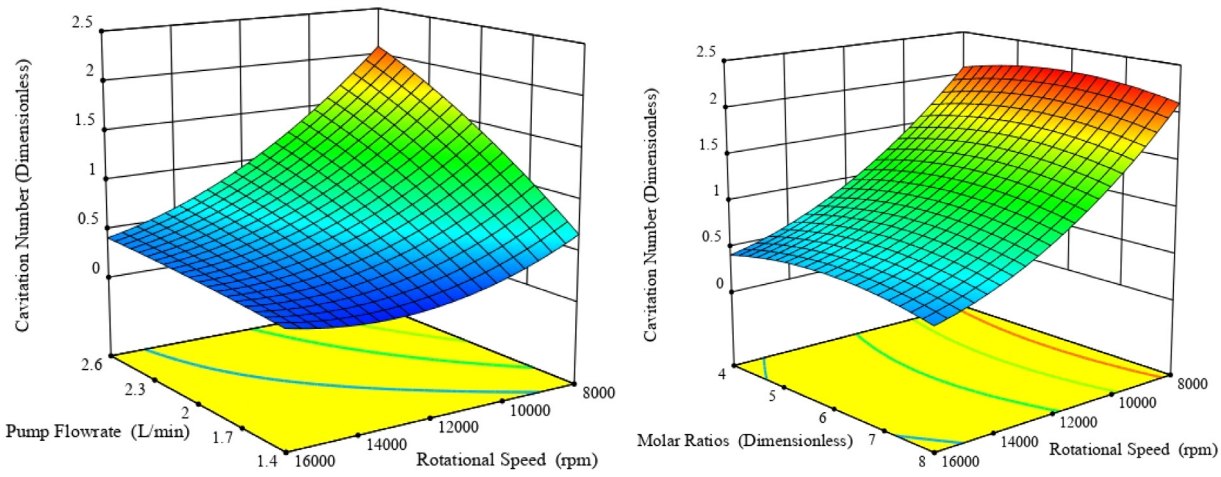

Fig. 3. Cavitation number of reactor related to the operating parameter (pump flow rate, methanol to oil molar ratio, rotational speed).

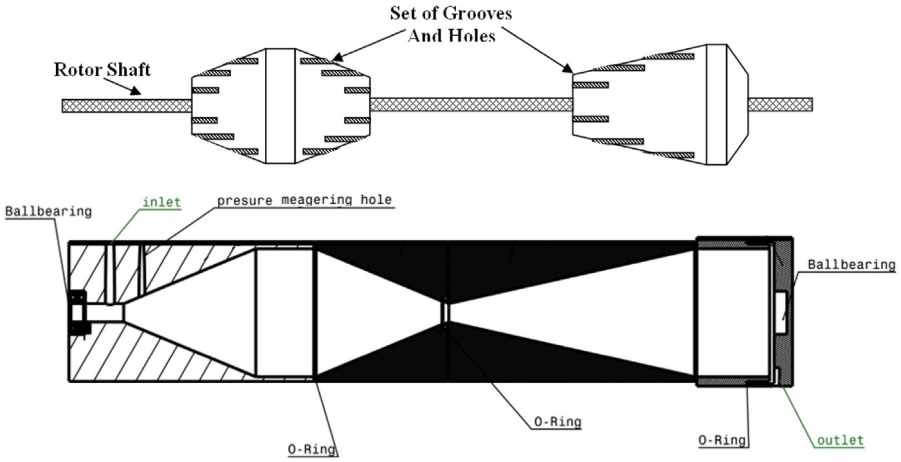

Fig. 4. The reactor rotor and stator.

where: σ = Cavitation number (dimensionless), p_r = reference pressure (Pa), p_v = vapor pressure of the fluid (Pa), ρ = density of the fluid (kg/m^3), and v = velocity of fluid

The cavitation number in the designed reactor changes due to the change in operating parameters. These changes are approximated by practical measurements and theoretical calculations in the Design Experts 11 software, which is in accordance with Fig. 3.

The cavitation number decreased with increasing rotational speed or decreasing pump flow rate, and vice versa. The changes in molar ratio and circulation time did not have a significant effect on the cavitation number. A drop in the cavitation number results in cavitation or an increase in the cavitation level (Šarc et al., 2017).

2.3. Application of hydrodynamic cavitation in biodiesel production

Among the technological innovations for biodiesel production, hydrodynamic cavitation is a high-potential method for producing biodiesel on an industrial scale that can be more easily developed (Pal et al., 2010b). The conversion of oil and alcohol to biodiesel by hydrodynamic cavitation is cheaper than traditional methods and its energy requirement is approximately half the amount of energy required by the conventional mechanical method.

In the hydrodynamic cavitation method, two phases of the reaction experience non-homogeneous pressure in a section of the reactor and the flow rate of the fluid becomes non-homogeneous due to the rotation in the path with a specific geometric dimension, leading to the formation of cavitation (Pal et al., 2010a). The velocity and pressure non-uniformity that generates pulses within the fluid can be created by a venturi or perforated plates embedded in the path of the fluid flow.

If the pressure of the venturi bottleneck is reduced to less than the evaporation pressure of the fluid flow, many holes are created throughout the fluid, and they increase the pressure and temperature of the pulses. These pulses lead to better mixing of heterogeneous fluids and increase the speed and efficiency of the transesterification reaction (Gogate and Pandit, 2005). The designed reactor, combines four features to increase the cavitation intensity.

(1) application of several holes in the reactor rotor (Simpson and Ranade, 2018b), (2) application of grooves parallel with the axis on the reactor rotor (Ozonek, 2011), (3) design of the reactor stator in the form of a venturi tube (Simpson and Ranade, 2018a), and (4) high speed rotation by high speed electromotor (Petkovšek et al., 2015; Sun et al., 2018). The flow through the openings of the single-hole or multi-hole plates increases the fluid velocity and decreases the pressure. The cavity intensity is directly related to the size of the plate hole (Ozonek, 2011; Pal et al., 2010b).

Fig. 4 shows an image of the venturi tube of the reactor stator and rotor. Fig. 5 shows an image of the cross-section of the reactor rotor with holes and grooves embedded in it.

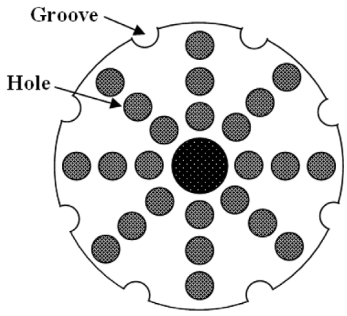

Fig. 5. The cross section of the reactor rotor with holes and grooves embedded on it.

Table 1
The results of comparing the properties of the produced biodiesel with the EN14214-08 standard.

Properties	Unit	Allowed limit	Measured value
Flash point	C°	101>	174
Kinematic viscosity C° 40	mm/s	5–3.5	3.93
Acid number	mg KOH/g	0.5<	0.41
Iodine number	g iodine/100 g	120<	97.56
Density C° 15	kg/m^3	900–860	868.315
Sulfated ash	%mass	0.020<	0.015
Oxidation stability	h	6>	6.11

3. Results

3.1. The results of examining the quality of the produced biodiesel

To ensure the quality of the produced biodiesel, the study measured some of its important properties with the aim of comparing it with the EN14214-08 standard (see Table 1). As shown in Table 1, the produced biodiesel met the relevant standards and could be reliably used in diesel engines.

Table 2 shows some of the characteristics of the conducted experiments. Thirty test specimens along with the used rapeseed oil (mL), the volume of methanol alcohol (mL), the molar ratio of methanol to oil (dimensionless), the rotational speed of the reactor (rpm), pump flow rate (L/min), circulation time (min), produced biodiesel volume (mL), the biodiesel yield and ER (dimensionless) are specified.

Table 3 shows the total value of input and output energies in the reaction of biodiesel production from rapeseed oil. The amounts of each input and output of the reaction and their equivalent energies are shown for producing a liter of biodiesel. The total amounts of input and output energies were 32.767 and 39.319 MJ/L. Fig. 6 shows the distribution of the consumption of different energy inputs for producing biodiesel. The lowest percentage was related to labor (0.24%), followed by electricity (0.65%), catalyst (0.72%), machinery (2.48%), methanol (22.57%), and rapeseed oil (73.35%). As can be seen, the most consumed energy was related to rapeseed oil.

Table 4 shows the average produced biodiesel and the energy ratio at different levels of the operating parameters. As seen in this table, by increasing the molar ratio from 4 to 6, the volumes of the produced biodiesel and biodiesel yield increased, and the energy ratio decreased slightly. But by increasing the molar ratio from 6 to 8, all three volumes of the produced biodiesel, biodiesel yield and energy ratio decreased. Also, as the rotational speed of the hydrodynamic reactor increased, the volumes of the produced biodiesel, biodiesel yield and energy ratio decreased. Hence, the rotational speed of 8000 rpm was the best.

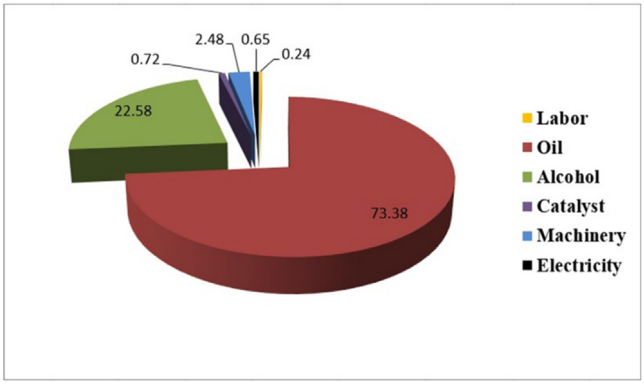

Fig. 6. The distribution of different energy inputs.

The molar ratio of alcohol to oil in terms of stoichiometric relations is 3:1, which requires long time to complete the transesterification reaction. As the molar ratio increases, the contact between alcohol and oil molecules increases (Lee and Saka, 2010) and also with more alcohol, the glycerin-fatty acid linkages is more easily broken. Miao and Wu (2006) On the other hand, more alcohol makes intensities cavitation that with formation of fine emulsions increases the rate of the reaction (Mohod et al., 2017). So, with the increase of the molar ratio, the biodiesel yield increases in a shorter time (Canoira et al., 2006; Helwani et al., 2009). However, the molar ratio of alcohol to oil greater than the optimal value, reduces the biodiesel yield, which is probably due to the increase in methanol in the reaction and increase the solubility of glycerin and prevents the process of glycerin separation from alkyl esters. Part of the diluted glycerin remains in alkyl esters and reduce the final product due to foam formation (Agarwal, 2007; Encinar et al., 2007; Rashid et al., 2008) and helps to reverse the reaction to the left (Verma and Sharma, 2016; Musa, 2016; Banerjee and Chakraborty, 2009; Mohod et al., 2017). It is even possible that an increase in methanol over an optimal value will result stronger of the catalyst leaching in the methanol and a decrease in biodiesel yield (Dwivedi and Sharma, 2015; Mohod et al., 2017).

The results also revealed that by increasing the pump flow rate from 1.4 to 2 L/min, the volumes of the produced biodiesel, biodiesel yield and energy ratio increased. By increasing the pump flow rate from 2 to 2.6 L/min, all three of these parameters decreased. Hence, the pump flow rate of 2 L/min was the best. The results demonstrated that with an increase in the circulation time from 2 to 4 min, the volumes of the produced biodiesel, biodiesel yield and energy ratio increased, and by increasing the circulation time from 4 to 6, these parameters decreased.

Finally, according to Table 4, the three operating parameters of molar ratio, pump flow rate and circulation time follow approximately the same law. In other words, by increasing the amount of these parameters, at first, the volumes of the produced biodiesel and biodiesel yield increased and then decreased.

Increasing the rotational speed caused the intensities cavitation and increased biodiesel yield, but by increasing the rotational speed from the optimal value, there is no significant effect on increasing the biodiesel yield but reduces its performance. In other words, increasing the rotational speed from the optimal value causes the formation of super cavitation, which causes the cushioned collapse phenomenon and reduces the overall effects of cavitation, which reduces the biodiesel yield (Joshi et al., 2017; Mohod et al., 2017).

As the pump flow rate increases, the speed of flow increases, resulting less residence time in the reactor, reducing the reactor's

Table 2
Some of the characteristics of the conducted experiments.

Run	Oil (mL)	Alcohol (mL)	Molar ratio	Speed (rpm)	Q (L/min)	Time (min)	Biodiesel (mL)	Biodiesel yield (v. %)	ER (dimensionless)
1	500	115	6	8000	2	4	424	84.89	1.219
2	500	154	8	8000	2.6	2	417	83.49	1.194
3	500	77	4	8000	2.6	2	415	83.03	1.251
4	500	77	4	16 000	2.6	2	410	81.99	1.239
5	500	154	8	8000	2.6	6	422	84.34	1.168
6	500	77	4	16 000	2.6	6	370	74.07	1.109
7	500	115	6	12 000	2	4	421	84.24	1.212
8	500	77	4	8000	2.6	6	425	85.01	1.233
9	500	115	6	12 000	2	4	419	83.74	1.206
10	500	154	8	16 000	2.6	2	422	84.40	1.202
11	500	115	6	12 000	2	4	424	84.74	1.218
12	500	115	6	12 000	2	4	425	84.99	1.221
13	500	115	6	12 000	2.6	4	437	87.33	1.242
14	500	115	6	16 000	2	4	445	88.94	1.258
15	500	115	6	12 000	2	4	417	83.49	1.203
16	500	154	8	16 000	1.4	6	371	74.11	1.083
17	500	115	6	12 000	1.4	4	426	85.18	1.221
18	500	77	4	8000	1.4	2	459	91.87	1.354
19	500	77	4	16 000	1.4	2	361	72.24	1.126
20	500	115	6	12 000	2	4	426	85.24	1.224
21	500	154	8	8000	1.4	2	458	91.57	1.263
22	500	154	8	16 000	2.6	6	372	74.50	1.086
23	500	77	4	16 000	1.4	6	390	77.92	1.153
24	500	77	4	8000	1.4	6	462	92.38	1.316
25	500	115	6	12 000	2	6	409	81.87	1.171
26	500	154	8	8000	1.4	6	422	84.49	1.169
27	500	154	8	16 000	1.4	2	425	84.99	1.207
28	500	115	6	12 000	2	2	386	77.23	1.161
29	500	77	4	12 000	2	4	421	84.15	1.243
30	500	154	8	12 000	2	4	429	85.73	1.196

Table 3
The energy consumption pattern for biodiesel production.

Input and output values	Unit	Amount per unit volume of biodiesel (L)	Total energy equivalent (MJ/L)
Labor	h	0.04	0.079
Rapeseed Oil	L	1.107	24.034
Alcohol (Methanol)	L	0.219	7.394
Catalyst (NaOH)	L	0.011	0.236
Electricity	kWh	0.017	0.213
Machinery	h	0.012	0.811
Total Input Energy	–	–	32.767
Biodiesel	L	1	32.780
Alcohol (Methanol)	L	0.179	6.053
Catalyst (NaOH)	L	0.011	0.236
Glycerin	L	0.009	0.250
Total output energy	–	–	39.319

Table 4
The average values of the produced biodiesel and energy ratio at different levels of the operating parameters.

		Biodiesel volume (mL)	Biodiesel yield (v. %)	ER (dimensionless)
The molar ratio of methanol to oil	4:1	412	82.52	1.225
	6:1	421	84.33	1.213
	8:1	415	83.07	1.174
The rotational speed of the reactor (rpm)	8000	433	86.79	1.241
	12 000	419	84.00	1.210
	16 000	396	79.24	1.162
Pump flow rate (L/min)	1.4	419	83.86	1.210
	2	420	84.11	1.211
	2.6	410	82.02	1.192
Circulation time (min)	2	417	83.42	1.222
	4	426	85.22	1.222
	6	404	80.97	1.165

effect and less conversion due to incomplete reaction, and ultimately reducing biodiesel yield. If the pump flow rate is lower, the residence time in the reactor will increase and the effect of the reactor and biodiesel yield will increase. However, before the optimal value of pump flow rate, due to the initial combination of oil and alcohol and incomplete reaction, the biodiesel yield is not maximum. Similar results were reported by Agarwal et al. (2013).

Circulating oil and alcohol is alone a simple mixing operation. The maximum duration of circulating in this study was 6 min, which is very low in the transesterification reaction, but because circulating causes the compound to pass through the reactor repeatedly, it can be said that the circulation intensifies the effect of the reactor. So, in high rotational speeds, increasing in the circulation time, causing super cavitation and reducing biodiesel yield.

As these parameters increase, the energy ratio is constantly decreasing due to the increase in input energy and, of course, the decrease in output energy due to the decrease in the volumes of the produced biodiesel and biodiesel yield. As rotational speed increases, the volume of the produced biodiesel, biodiesel yield and energy ratio decrease, which can be due to the increased cavitation and reversibility of biodiesel production reaction and increased electricity consumption.

The average value of the energy ratio in biodiesel production from rapeseed oil was calculated at 1.205, which was more than one, an indication that output energy was greater than input energy, and; in other words, the energy has been generated in this reaction. The reaction of biodiesel production was logically and scientifically correct in the present research. In a study done by Abshar and Sami (2016), the energy ratio of biodiesel production from rapeseed oil was evaluated and it was obtained at 1.08. In a study, Mohammadshirazi et al. (2014) analyzed the energy of biodiesel produced from waste oil using the mechanical mixing method and estimated the energy ratio was obtained at 1.49. In another study, Naderloo et al. (2017) used the ANFIS method to produce biodiesel from waste oil in an ultrasonic reactor and calculated the energy ratio at 1.28.

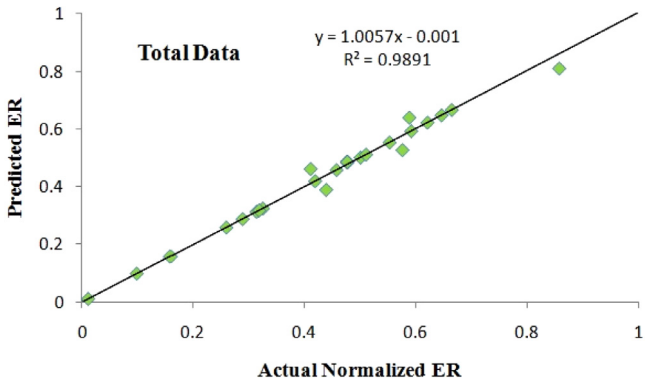

Fig. 7. The graph of the real and predicted values of the ANFIS model.

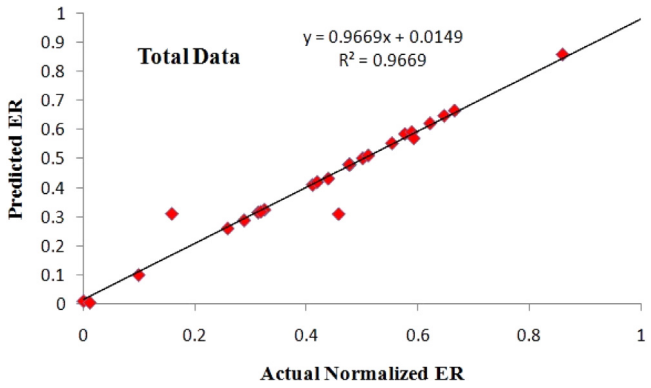

Fig. 8. The graph of the real and predicted values of the ANN model.

3.2. Modeling and studying the energy ratio of biodiesel

The inputs of the models included four items: pump flow rate, the molar ratio of oil to alcohol, rotational speed and circulation time, and the output of the models was the ER of biodiesel production. Due to the different scales of the inputs relative to each other, all normalized inputs and outputs were used for the correct operation of the smart models. Also, in all models, 30% and 70% of the data were used for testing and training.

3.2.1. Modeling through ANFIS

The ANFIS fuzzy inference system is a combination of fuzzy systems and artificial neural networks, with the benefits of both (Metin Ertunc and Hosoz, 2008; Buragohain and Mahanta, 2008). This system is useful for solving nonlinear problems that are very complicated (Cheng et al., 2002). ANFIS is capable of establishing and deducing non-linear relationships between inputs and outputs using linguistic concepts (Guillaume, 2001; Naderloo et al., 2012). Five key factors that were optimized in the ANFIS model are as follows: the type of input fuzzy sets, the number of fuzzy input sets, the type of output fuzzy sets, the optimization method, and the number of epochs. In the best model obtained using the ANFIS model, there were three fuzzy sets for each input and their type was gauss2mf. The output of the model and the optimization method was linear and hybrid, and there were 60 epochs. The normalized actual ER versus predicted ER for the best ANFIS model is shown in Fig. 7.

3.2.2. Modeling through artificial neural network

Artificial neural networks are used for solving complex problems, a method similar to that of human brain function. According to the results of studies conducted on the mechanism and structure of the human brain, neural networks can be used as a new computing technology for solveing complex problems such as pattern recognition, classification, and prediction. In this research, a network with a multi-layered perceptron model was selected, and in the best model of the neural network, the Tansig–Purelin transfer function was used in the first and second layers. The training function was Levenberg–Marquardt, and the network structure was 4×1. The normalized actual ER versus predicted ER for the best ANN model is shown in Fig. 8.

3.2.3. Modeling through response surface methodology (RSM)

The response surface methodology is a set of mathematical and statistical techniques used for developing, promoting and optimizing processes in which the intended level is affected by many variables, and the goal is to optimize the response. In this study, the Design Expert 11 software was used for this aim. The model obtained from the RSM method was Cubic. The normalized actual ER versus predicted ER for the best RSM model is shown in Fig. 9.

Table 5
The performance of the best model derived from the three methods.

Model type		TSE[a]	MAE[b]	MSE	R^2	p-value
ANFIS	Train	0.0002	0.0013	9.93E−06	0.999	3.7E−36
	Test	0.0152	0.0362	0.0016	0.957	4.73E−06
	Total	0.0154	0.0117	0.0005	0.989	5.01E−29
ANN	Train	0.0230	0.0095	0.0010	0.977	4.95E−17
	Test	0.0226	0.0203	0.0025	0.957	4.56E−06
	Total	0.0456	0.0128	0.0015	0.966	2.88E−22
RSM	Train	0.0009	0.0063	4.34E−05	0.990	7.56E−21
	Test	9.13E−05	0.003184	1.01E−05	0.932	2.42E−05
	Total	0.0010	0.0053	3.34E−05	0.9901	1.19E−29

[a]Total Squared Error.
[b]Mean Absolute Error.

4. Discussion

4.1. Comparing the three models designed for ER

The author used three indexes to compare and evaluate the three models obtained from the ANFIS, ANN and RSM methods: (1) comparison of the determination coefficients (R^2) and mean squared errors (MSE) of models, (2) comparison of the residuals of models, and (3) simplicity and speed of models. Table 5 shows the characteristics of the models derived from the three methods.

As shown in Table 5, the MSE and R^2 of the ANFIS model at the testing step were 0.0017 and 0.957. In a study (Naderloo et al., 2017), the ER of biodiesel production from waste oil in an ultrasonic reactor was modeled by the ANFIS method, and the results demonstrated that the MSE and R^2 of the ANFIS model at the testing step were 5×10^{-6} and 0.87. In comparison, it can be stated that the R^2 of the present model was higher. As seen in Table 5, the MSE and R^2 of the ANFIS model were 0.0005 and 0.989 for the whole data. The same factors were 0.0015 and 0.966 for the ANN model and 0.00003 and 0.990 for the RSM model. In a study (Mostafaei et al., 2016), the value of R^2 for modeling the effects of reactor size and ultrasonic power on the biodiesel production efficiency in the ANFIS model was estimated at 0.981, which was higher than that in the RSM method (0.967).

The model is better when it has a higher R^2 value and lower MSE value. As shown in Fig. 10, the model derived from the RSM was better. The other index for the evaluation of the models is their residual graph. In the residual graph, the proximity of the error curve to the horizontal axis shows the good performance of the model. As a result, according to Fig. 11, the RSM model was better.

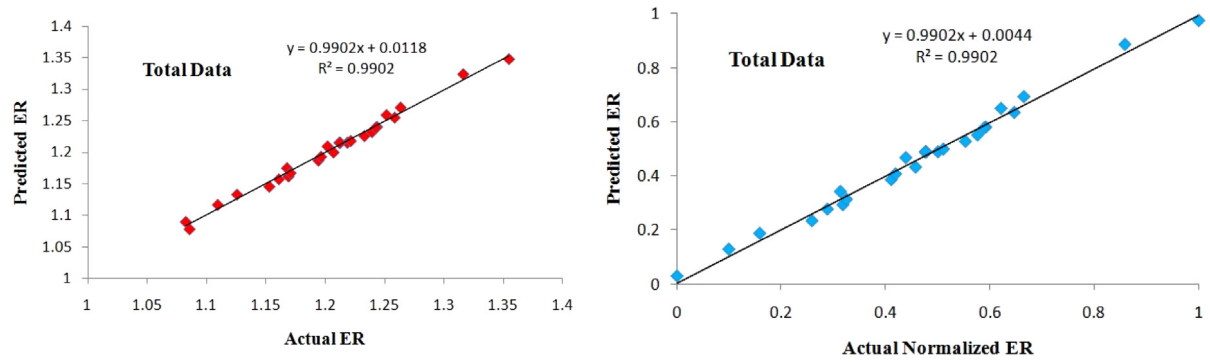

Fig. 9. The graph of the real and predicted values of the RSM model (normalized values: right; real values: left).

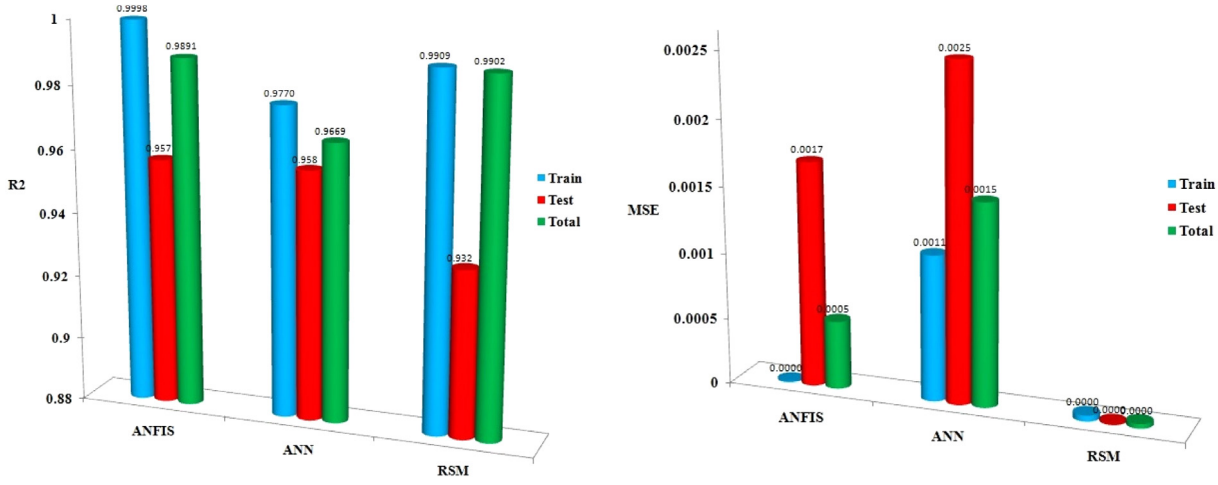

Fig. 10. The values of the R^2 (left) and MSE (right) of training, testing and the whole data.

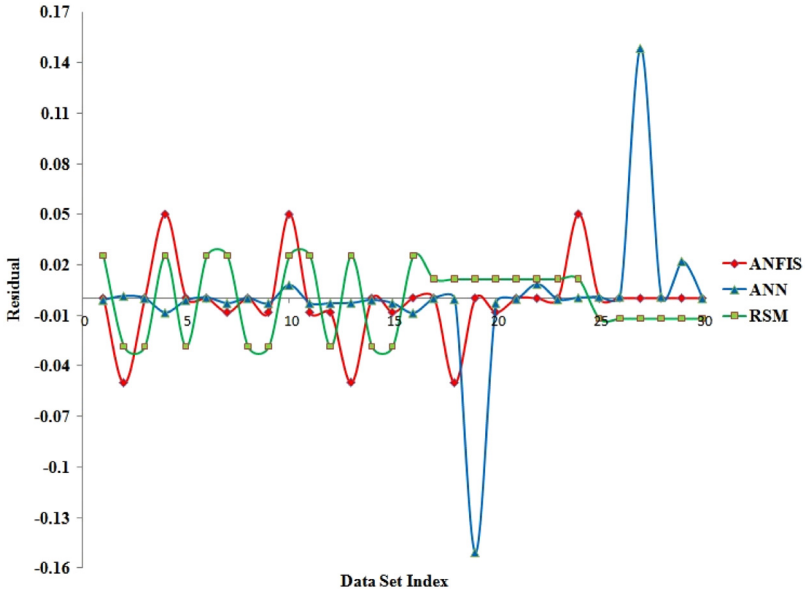

Fig. 11. The residual graphs of ANFIS, ANN and RSM models.

4.1.1. Desirability function

In modeling by different methods and techniques, usually come up with the model's several different features, which make it difficult to compare and select the best method because of the proximity of the features. The desirability function is a practical and suitable function for summarizing the features among different methods and choosing the best one based on the numerical evaluation. The output of the desirability function is a value between zero and one, and the closer output to one is better. Eqs. (3) to (5) show the desirability function (sarve et al., 2015;

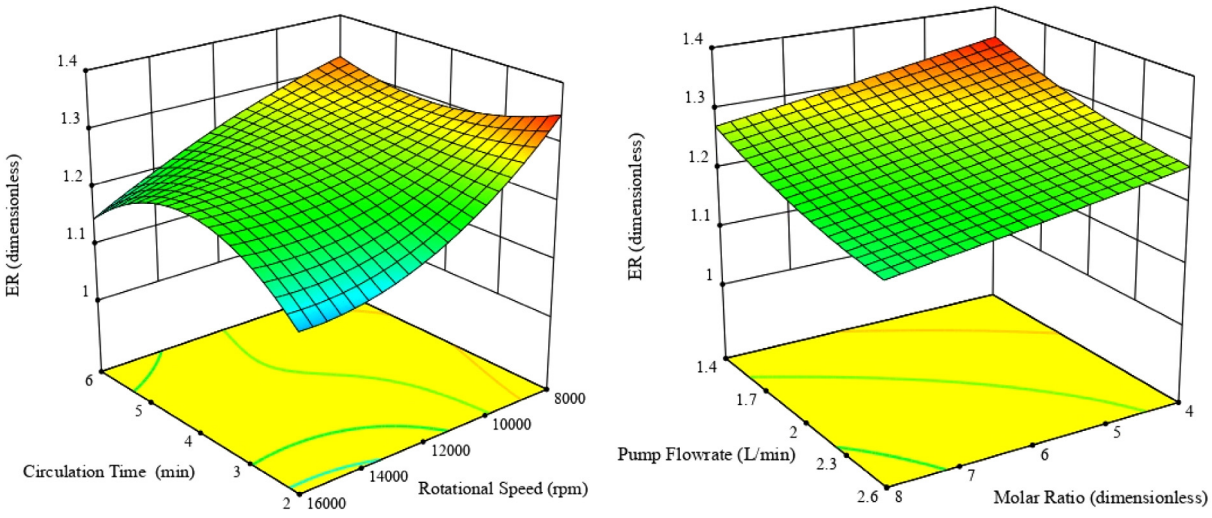

Fig. 12. The effects of various settings of the reactor on the energy ratio.

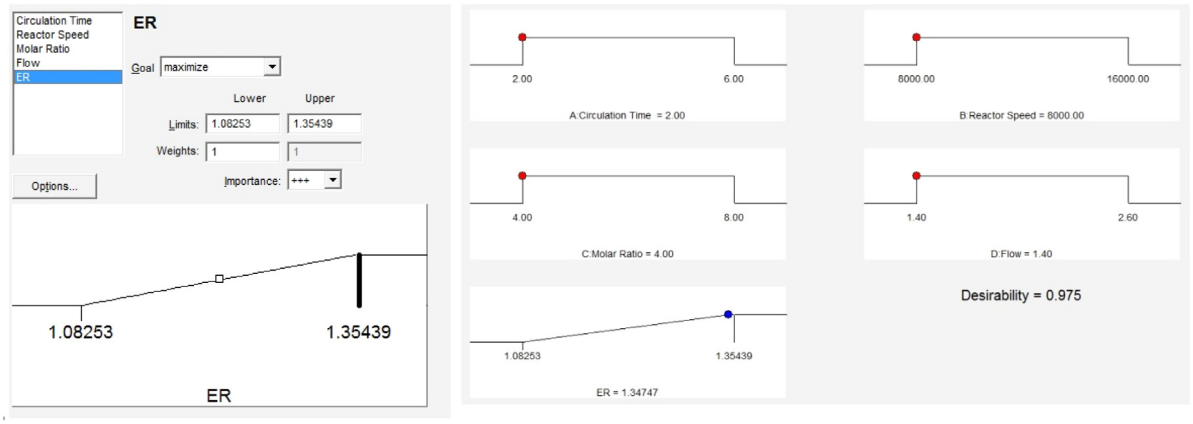

Fig. 13. The optimization window of the RSM model to find the maximum energy ratio (right), reactor settings to achieve the maximum energy ratio (left).

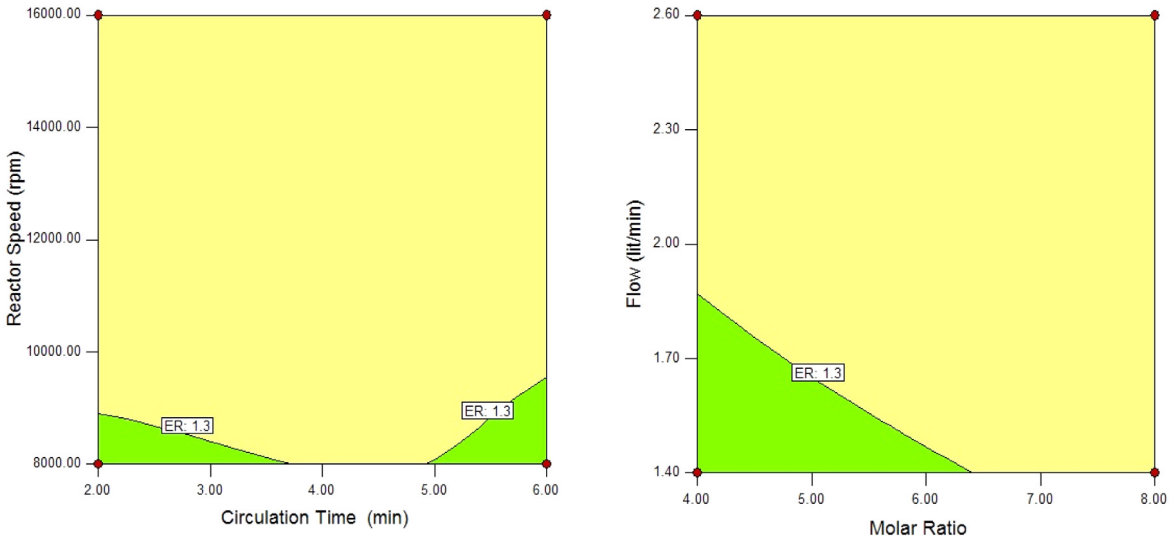

Fig. 14. The reactor settings to get energy ratio greater than 1.3.

Vera Candioti et al., 2014).

$$d_{imax} = \frac{y - L}{U - L} \quad (3)$$

$$d_{imin} = \frac{U - y}{U - L} \quad (4)$$

$$D_{final} = (d_1 \times d_2 \times \cdots \times d_n)^{1/n} \quad (5)$$

Table 6
Investigation of different features of desirability function in three models.

Model	Feature 1		Feature 2		Feature 3		D_{final}
	R^2	d_{1max}	MSE	d_{2min}	TSE	d_{3min}	
ANFIS	0.989	0.95	0.0005	0.67	0.0154	0.67	0.75
ANN	0.966	0	0.0015	0	0.0456	0	0
RSM	**0.990**	**1**	**3.34E−05**	**1**	**0.0010**	**1**	**1**

where n is the number of evaluating indexes, U is the maximum value of the feature among different methods, L is the minimum value of the feature among different methods, y is the evaluating feature, d_{imax} is an index that the maximum value of the evaluating feature is better, d_{imin} is the index that the minimum value of the evaluating feature is better, and D_{final} is the final result of desirability function. Based on the results of Table 6, the best model is RSM.

4.2. Examining the performance of the best model

Due to the excellent performance of the RSM model, it was examined more accurately and used for finding the best performance conditions for the reactor. In the non-normalized model of all parameters, the effects of variations on the output of the model can be better examined (see Fig. 12).

Fig. 12 shows the effects of the changes in the input parameters on the ER. To find the reactor settings for maximizing the ER, it is enough to find the maximum point in the model graph. For this purpose, as shown in Fig. 13 (left), the output of the model (ER) was set to the maximum value. The final results from the optimization of the model are shown in Fig. 13. In this figure, the maximum ER occurs when the circulation time, rotational speed, the pump flow rate and the molar ratio are set in 2 min, 8000 rpm, 1.4 L/min and 4, respectively. Fig. 14 displays the reactor settings to obtain an ER higher than 1.3. The ER in the green zone was more than 1.3 and in the yellow zone was less than it.

Fig. 15 shows the effect of the ER changes versus impure biodiesel yield. The impure biodiesel consists of pure biodiesel with catalysts, alcohols and glycerin. The maximum biodiesel yield in this research was 92.38%. The produced impure biodiesel should be washed before consumption. The pure biodiesel obtained in this study was more than 98% yield after washing according to the EN 14214 standard. In other words, in this study, the settings of the designed reactor were optimized based on the ER. The output of the reactor is impure biodiesel, so it is necessary to consider it instead of the pure biodiesel (output of the reactor along with the washing process) in modeling and analyzing. As shown in Fig. 15, by increasing the impure biodiesel yield, the ER usually increases. But it unusually reduces somewhere because the ER depends on two factors according to Eq. (1). It has a direct relationship with the total output energy (highly dependent on the impure biodiesel yield) and an inverse relationship with the total input energy. Although the numerator increased through increasing the impure biodiesel yield and output energy, the denominator, which is the sum of the input energies, further increased, and the ER is reduced.

5. Conclusion

In the present study, a hydrodynamic cavitation reactor was mechanized for the production of biodiesel by the transesterification method. The user-friendly controller of the reactor was designed by the LabVIEW Version 2016 and USB-DAQ-6009 Card and equipped with electric valves and temperature sensors. To find the best settings of the reactor for biodiesel production in terms of ER, the study modeled the reactor's performance based on its settings and employed ANFIS, ANN and RSM methods for modeling. Rapeseed oil, with different molar ratios of methanol to oil and sodium hydroxide catalyst were used in the reactor for biodiesel production.

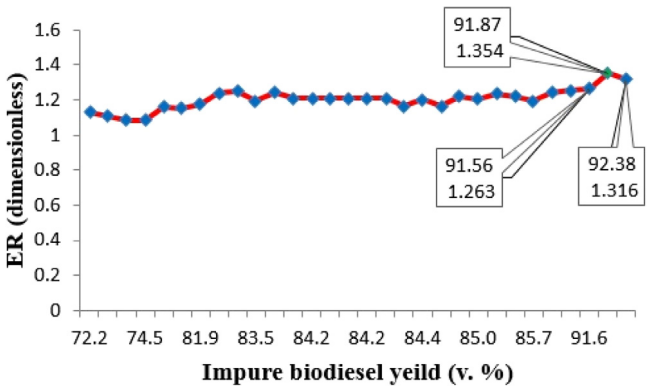

Fig. 15. The energy ratio changes due to the impure biodiesel yield changes.

The inputs of the models included four items: pump flow rate, the molar ratio of methanol to oil, rotational speed and circulation time. The output of the models was the ER. The results showed the R^2 of the best ANFIS, ANN and RSM models were 0.989, 0.966, and 0.990, respectively. The MSE of the best ANFIS, ANN and RSM models were obtained at 0.0005, 0.0015 and 0.00003, respectively. The results revealed that the RSM and ANFIS models were preferred to the ANN model in terms of better performance, simplicity, and high processing speed. In total, the RSM model was better than the ANFIS model based on the desirability function. Accordingly, the best reactor settings to obtain the maximum ER (1.35) and biodiesel yield (91.87%) were when the circulation time, the rotational speed, the pump flow rate and the molar ratio were 2 min, 8000 rpm, 1.4 L/min and 4, respectively.

CRediT authorship contribution statement

Leila Naderloo: Conceptualization, Methodology, Software, Validation, Formal analysis, Investigation, Resources, Data curation, Writing - original draft, Writing - review & editing.

Declaration of competing interest

The authors declare that they have no known competing financial interests or personal relationships that could have appeared to influence the work reported in this paper.

Acknowledgments

The author would like to acknowledge the financial support from Ministry of Science, Research and Technology, Tehran, Iran and the Vice Chancellor for Research and Technology of Razi University, Iran.

References

Abshar, R., Sami, M., 2016. Evaluation energy efficiency in biodiesel production from Canola A case study. J. Life Sci. Biomed. 6 (3), 71–75.

Agarwal, A.K., 2007. Biofuels (alcohols and biodiesel) applications as fuels for internal combustion engines. Prog. Energy Combust. Sci. 33 (3), 233–271. http://dx.doi.org/10.1016/j.pecs.2006.08.003.

Agarwal, M., Soni, S., Singh, K., Chaurasia, S.P., Dohare, R.K., 2013. Biodiesel yield assessment in continuous-flow reactors using batch reactor conditions. Int. J. Green Energy 10 (1), 28–40. http://dx.doi.org/10.1080/15435075.2011.647171.

Asif, S., Ahmad, M., Bokhari, A., Chuah, L.F., Klemeš, J.J., Akbar, M.M., Sultana, S., Yusup, S., 2017a. Methyl ester synthesis of Pistacia khinjuk seed oil by ultrasonic-assisted cavitation system. Ind. Crops Prod. 108, 336–347. http://dx.doi.org/10.1016/j.indcrop.2017.06.046.

Asif, S., Chuah, L.F., Klemeš, J.J., Ahmad, M., Akbar, M.M., Lee, K.T., Fatima, A., 2017b. Cleaner production of methyl ester from non-edible feedstock by ultrasonic-assisted cavitation system. J. Cleaner Prod. 161, 1360–1373. http://dx.doi.org/10.1016/j.jclepro.2017.02.081.

Banerjee, A., Chakraborty, R., 2009. Parametric sensitivity in transesterification of waste cooking oil for biodiesel production—A review. Resour. Conserv. Recycl. 53 (9), 490–497. http://dx.doi.org/10.1016/j.resconrec.2009.04.003.

Bokhari, A., Yusup, S., Chuah, L.F., Klemeš, J.J., Asif, S., Ali, B., Akbar, M.M., Kamil, R.N.M., 2017. Pilot scale intensification of rubber seed (Hevea brasiliensis) oil via chemical interesterification using hydrodynamic cavitation technology. Bioresour. Technol. 242, 272–282. http://dx.doi.org/10.1016/j.biortech.2017.03.046.

Buragohain, M., Mahanta, C., 2008. A novel approach for ANFIS modelling based on full factorial design. Appl. Soft Comput. 8 (1), 609–625. http://dx.doi.org/10.1016/j.asoc.2007.03.010.

Canoira, L., Alcántara, R., Jesús García-Martínez, M., Carrasco, J., 2006. Biodiesel from Jojoba oil-wax: Transesterification with methanol and properties as a fuel. Biomass Bioenergy 30 (1), 76–81. http://dx.doi.org/10.1016/j.biombioe.2005.07.002.

Cheng, C.-B., Cheng, C.J., Lee, E.S., 2002. Neuro-fuzzy and genetic algorithm in multiple response optimization. Comput. Math. Appl. 44 (12), 1503–1514. http://dx.doi.org/10.1016/S0898-1221(02)00274-2.

Chuah, L.F., Klemeš, J.J., Yusup, S., Bokhari, A., Akbar, M.M., Chong, Z.K., 2017. Kinetic studies on waste cooking oil into biodiesel via hydrodynamic cavitation. J. Cleaner Prod. 146, 47–56. http://dx.doi.org/10.1016/j.jclepro.2016.06.187.

Dayhoff, J., 1990. Neural Network Principles. Prentice-Hall International, U.S.A.

Demirbas, A., 2009. Biofuels from agricultural biomass. Energy Sources A 31 (17), 1573–1582.

Dwivedi, G., Sharma, M.P., 2015. Application of Box–Behnken design in optimization of biodiesel yield from Pongamia oil and its stability analysis. Fuel 145, 256–262. http://dx.doi.org/10.1016/j.fuel.2014.12.063.

Encinar, J.M., González, J.F., Rodríguez-Reinares, A., 2007. Ethanolysis of used frying oil. Biodiesel preparation and characterization.. Fuel Process. Technol. 88 (5), 513–522. http://dx.doi.org/10.1016/j.fuproc.2007.01.002.

Esengun, K., Gündüz, O., Erdal, G., 2007. Input–output energy analysis in dry apricot production of Turkey. Energy Convers. Manage. 48 (2), 592–598. http://dx.doi.org/10.1016/j.enconman.2006.06.006.

Farkas, I., Reményi, P., Biró, A., 2000. A neural network topology for modelling grain drying. Comput. Electron. Agric. 26 (2), 147–158. http://dx.doi.org/10.1016/S0168-1699(00)00068-5.

Gerpen, J.V., 2005. Biodiesel processing and production. Fuel Process. Technol. 86 (10), 1097–1107.

Gogate, P.R., Pandit, A.B., 2005. A review and assessment of hydrodynamic cavitation as a technology for the future. Ultrason. Sonochemistry 12 (1), 21–27. http://dx.doi.org/10.1016/j.ultsonch.2004.03.007.

Guillaume, S., 2001. Designing fuzzy inference systems from data: An interpretability-oriented review. Trans. Fuzzy Syst. 9 (3), 426–443. http://dx.doi.org/10.1109/91.928739.

Helwani, Z., Othman, M.R., Aziz, N., Fernando, W.J.N., Kim, J., 2009. Technologies for production of biodiesel focusing on green catalytic techniques: A review. Fuel Process. Technol. 90 (12), 1502–1514. http://dx.doi.org/10.1016/j.fuproc.2009.07.016.

Hosseinpour, S., Aghbashlo, M., Tabatabaei, M., Khalife, E., 2016. Exact estimation of biodiesel cetane number (CN) from its fatty acid methyl esters (FAMEs) profile using partial least square (PLS) adapted by artificial neural network (ANN). Energy Convers. Manage. 124, 389–398. http://dx.doi.org/10.1016/j.enconman.2016.07.027.

Jafari, R., Niknejad, Y., Fallah, H., 2015. Assess the energy efficiency of rapeseed (Brassica napus L.) Production in the Mazandaran province: A case study of Amol city. Biol. Forum - Int. J. 7 (1), 1143–1148.

Ji, J., Wang, J., Li, Y., Yu, Y., Xu, Z., 2006. Preparation of biodiesel with the help of ultrasonic and hydrodynamic cavitation. Ultrasonics 44, e411–e414. http://dx.doi.org/10.1016/j.ultras.2006.05.020.

Joshi, S., Gogate, P.R., Moreira, P.F., Giudici, R., 2017. Intensification of biodiesel production from soybean oil and waste cooking oil in the presence of heterogeneous catalyst using high speed homogenizer. Ultrason. Sonochemistry 39, 645–653. http://dx.doi.org/10.1016/j.ultsonch.2017.05.029.

Ju, X.T., Kou, C.L., Zhang, F.S., Christie, P., 2006. Nitrogen balance and groundwater nitrate contamination: Comparison among three intensive cropping systems on the North China Plain. Environ. Pollut. 143 (1), 117–125. http://dx.doi.org/10.1016/j.envpol.2005.11.005.

Kelkar, M.A., Gogate Pr Fau - Pandit, A.B., Pandit, A.B., Intensification of esterification of acids for synthesis of biodiesel using acoustic and hydrodynamic cavitation. (1350-4177 (Print)).

Kent, J.A., 2013. Handbook of Industrial Chemistry and Biotechnology. Springer Science & Business Media.

Khanna, T., 1990. Foundation of Neural Networks (Addison-Wesley Series in New Horizons in Technology). Addison-Wesley Publishing Company, U.S.A.

Lee, J.-S., Saka, S., 2010. Biodiesel production by heterogeneous catalysts and supercritical technologies. Bioresour. Technol. 101 (19), 7191–7200. http://dx.doi.org/10.1016/j.biortech.2010.04.071.

Mandal, K.G., Saha, K., Ghosh, P.K., Hati, K., Bandyopadhyay, K., 2002. Bioenergy and Economic Analysis of Soybean-Based Crop Production Systems in Central India, Vol 23. http://dx.doi.org/10.1016/S0961-9534(02)00058-2.

Metin Ertunc, H., Hosoz, M., 2008. Comparative analysis of an evaporative condenser using artificial neural network and adaptive neuro-fuzzy inference system. Int. J. Refrig. 31 (8), 1426–1436. http://dx.doi.org/10.1016/j.ijrefrig.2008.03.007.

Miao, X., Wu, Q., 2006. Biodiesel production from heterotrophic microalgal oil. Bioresour. Technol. 97 (6), 841–846. http://dx.doi.org/10.1016/j.biortech.2005.04.008.

Miraboutalebi, S.M., Kazemi, P., Bahrami, P., 2016. Fatty Acid Methyl Ester (FAME) composition used for estimation of biodiesel cetane number employing random forest and artificial neural networks: A new approach. Fuel 166, 143–151. http://dx.doi.org/10.1016/j.fuel.2015.10.118.

Mohadesi, M., Aghel, B., Khademi, M.H., Sahraei, S., 2017. Optimization of biodiesel production process in a continuous microchannel using response surface methodology. Korean J. Chem. Eng. 34 (4), 1013–1020. http://dx.doi.org/10.1007/s11814-016-0342-9.

Mohammadi, A., Rafiee, S., Mohtasebi, S.S., Rafiee, H., 2010. Energy inputs – yield relationship and cost analysis of kiwifruit production in Iran. Renew. Energy 35 (5), 1071–1075. http://dx.doi.org/10.1016/j.renene.2009.09.004.

Mohammadshirazi, A., Akram, A., Rafiee, S., Bagheri Kalhor, E., 2014. Energy and cost analyses of biodiesel production from waste cooking oil. Renew. Sustain. Energy Rev. 33, 44–49. http://dx.doi.org/10.1016/j.rser.2014.01.067.

Mohod, A.V., Gogate, P.R., Viel, G., Firmino, P., Giudici, R., 2017. Intensification of biodiesel production using hydrodynamic cavitation based on high speed homogenizer. Chem. Eng. J. 316, 751–757. http://dx.doi.org/10.1016/j.cej.2017.02.011.

Mostafaei, M., Javadikia, H., Naderloo, L., 2016. Modeling the effects of ultrasound power and reactor dimension on the biodiesel production yield: Comparison of prediction abilities between response surface methodology (RSM) and adaptive neuro-fuzzy inference system (ANFIS). Energy 115, 626–636. http://dx.doi.org/10.1016/j.energy.2016.09.028.

Musa, I.A., 2016. The effects of alcohol to oil molar ratios and the type of alcohol on biodiesel production using transesterification process. Egypt. J. Pet. 25 (1), 21–31. http://dx.doi.org/10.1016/j.ejpe.2015.06.007.

Naderloo, L., Alimardani, R., Omid, M., Sarmadian, F., Javadikia, P., Torabi, M.Y., Alimardani, F., 2012. Application of ANFIS to predict crop yield based on different energy inputs. Measurement 45 (6), 1406–1413. http://dx.doi.org/10.1016/j.measurement.2012.03.025.

Naderloo, L., Javadikia, H., Mostafaei, M., 2017. Modeling the energy ratio and productivity of biodiesel with different reactor dimensions and ultrasonic power using ANFIS. Renew. Sustain. Energy Rev. 70, 56–64. http://dx.doi.org/10.1016/j.rser.2016.11.035.

Nguyen, T.L., Gheewala Sh Fau - Garivait, S., 0000. Garivait S Full chain energy analysis of fuel ethanol from cassava in Thailand. (0013-936X (Print)).

Ozonek, J.K.L., 2011. Effect of different design features of the reactor on hydrodynamic cavitation process. Arch. Mater. Sci. Eng. 52 (2), 112–117.

Pal, A., Verma, A., Kachhwaha, S., Maji, S., 2010a. Biodiesel Production Through Hydrodynamic Cavitation and Performance Testing, Vol. 35. http://dx.doi.org/10.1016/j.renene.2009.08.027.

Pal, A., Verma, A., Kachhwaha, S., Maji, S., 2010b. Biodiesel production through hydrodynamic cavitation and performance testing. Renew. Energy 35 (3), 619–624.

Papong, S., Chom-In, T., Noksa-nga, S., Malakul, P., 2010. Life cycle energy efficiency and potentials of biodiesel production from palm oil in Thailand. Energy Policy 38 (1), 226–233. http://dx.doi.org/10.1016/j.enpol.2009.09.009.

Petkovšek, M., Mlakar, M., Levstek, M., Stražar, M., Širok, B., Dular, M., 2015. A novel rotation generator of hydrodynamic cavitation for waste-activated sludge disintegration. Ultrason. Sonochemistry 26, 408–414. http://dx.doi.org/10.1016/j.ultsonch.2015.01.006.

Piloto-Rodríguez, R., Sánchez-Borroto, Y., Lapuerta, M., Goyos-Pérez, L., Verhelst, S., 2013. Prediction of the cetane number of biodiesel using artificial neural networks and multiple linear regression. Energy Convers. Manage. 65, 255–261. http://dx.doi.org/10.1016/j.enconman.2012.07.023.

Rashid, U., Anwar, F., Moser, B.R., Ashraf, S., 2008. Production of sunflower oil methyl esters by optimized alkali-catalyzed methanolysis. Biomass Bioenergy 32 (12), 1202–1205. http://dx.doi.org/10.1016/j.biombioe.2008.03.001.

Saiki, T., Karaki, I., Roy, K., 1999. CIGR Handbook of Agricultural Engineering, Vol. VI.

Šarc, A., Stepišnik-Perdih, T., Petkovšek, M., Dular, M., 2017. The issue of cavitation number value in studies of water treatment by hydrodynamic cavitation. Ultrason. Sonochemistry 34, 51–59. http://dx.doi.org/10.1016/j.ultsonch.2016.05.020.

sarve, A., Varma, M., Sonawane, S., 2015. Response surface optimization and Artificial neural network modeling of biodiesel production from crude Mahua (Madhuca indica) oil under supercritical ethanol condition using CO2 as co-solvent. RSC Adv. 5. http://dx.doi.org/10.1039/C5RA11911A.

Simpson, A., Ranade, V.V., 2018a. Modeling hydrodynamic cavitation in venturi: Influence of venturi configuration on inception and extent of cavitation. AIChE J. 0 (ja), http://dx.doi.org/10.1002/aic.16411.

Simpson, A., Ranade, V.V., 2018b. Modelling of hydrodynamic cavitation with orifice: Influence of different orifice designs. Chem. Eng. Res. Des. 136, 698–711. http://dx.doi.org/10.1016/j.cherd.2018.06.014.

Singh, J.M., 2002. On Farm Energy Use Pattern in Different Cropping Systems in Haryana. Flensburg State Univ., Germany, India.

Singh, S., Mittal, J.P., 1992. Energy in Production Agriculture. Mittol Pub, New Delhi.

Singhal, A.K., Athavale, M.M., Li, H., Jiang, Y., 2002. Mathematical basis and validation of the full cavitation model. J. Fluids Eng. 124 (3), 617–624. http://dx.doi.org/10.1115/1.1486223.

Sun, X., Park, J.J., Kim, H.S., Lee, S.H., Seong, S.J., Om, A.S., Yoon, J.Y., 2018. Experimental investigation of the thermal and disinfection performances of a novel hydrodynamic cavitation reactor. Ultrason. Sonochemistry 49, 13–23. http://dx.doi.org/10.1016/j.ultsonch.2018.02.039.

Vera Candioti, L., De Zan, M., Cámara, M., Goicoechea, H., 2014. Experimental design and multiple response optimization. Using the desirability function in analytical methods development. Talanta 124, 123–138. http://dx.doi.org/10.1016/j.talanta.2014.01.034.

Verma, P., Sharma, M.P., 2016. Comparative analysis of effect of methanol and ethanol on Karanja biodiesel production and its optimisation. Fuel 180, 164–174. http://dx.doi.org/10.1016/j.fuel.2016.04.035.